

# A novel approach to investigate the effect of methionine oxidation on pharmacokinetic properties of therapeutic antibodies

Jan Stracke<sup>1,2,\*</sup>, Thomas Emrich<sup>3</sup>, Petra Rueger<sup>1</sup>, Tilman Schlothauer<sup>1</sup>, Lothar Kling<sup>3</sup>, Alexander Knaupp<sup>1</sup>, Hubert Hertenberger<sup>1</sup>, Andreas Wolfert<sup>3</sup>, Christian Spick<sup>1</sup>, Wilma Lau<sup>1</sup>, Georg Drabner<sup>1</sup>, Ulrike Reiff<sup>1</sup>, Hans Koll<sup>1</sup>, and Apollon Papadimitriou<sup>3</sup>

<sup>1</sup>Biochemical and Analytical Research; Large Molecule Research; Roche Pharma Research and Early Development (pRED); Roche Innovation Center; Penzberg, Germany;

<sup>2</sup>Pharmaceutical Development & Supplies; Pharma Technical Development Biologics Europe; F. Hoffmann-La Roche Ltd.; Basel, Switzerland;

<sup>3</sup>Large Molecule Bioanalytical Research & Development; Pharmaceutical Sciences; Roche Pharma Research and Early Development (pRED);

Roche Innovation Center; Penzberg, Germany

**Keywords:** Antibody, FcRn, neonatal Fc receptor, methionine oxidation, degradation, Met252, Met428, pharmacokinetics, affinity chromatography, column, pH gradient

**Abbreviations:** AUC, area under the concentration-time curve; ESI-MS, electrospray ionization mass spectrometry; Fab, antigen-binding fragment; Fc, crystallizable fragment; FcRn, neonatal Fc receptor; HRP, horseradish peroxidase; IgG, immunoglobulin G; mAb, monoclonal antibody; Met, methionine; m/z, mass-to-charge ratio; PK, pharmacokinetic; RU, response units; SEC, size exclusion chromatography; SPR, surface plasmon resonance.

Preserving the chemical and structural integrity of therapeutic antibodies during manufacturing and storage is a major challenge during pharmaceutical development. Oxidation of Fc methionines Met252 and Met428 is frequently observed, which leads to reduced affinity to FcRn and faster plasma clearance if present at high levels. Because oxidation occurs in both positions simultaneously, their individual contribution to the concomitant changes in pharmacokinetic properties has not been clearly established. A novel pH-gradient FcRn affinity chromatography method was applied to isolate three antibody oxidation variants from an oxidized IgG1 preparation based on their FcRn binding properties. Physico-chemical characterization revealed that the three oxidation variants differed predominantly in the number of oxMet252 per IgG (0, 1, or 2), but not significantly in the content of oxMet428. Corresponding to the increase in oxMet252 content, stepwise reduction of FcRn affinity *in vitro*, as well as faster clearance and shorter terminal half-life, in huFcRn-transgenic mice were observed. A single Met252 oxidation per antibody had no significant effect on pharmacokinetics (PK) compared with unmodified IgG. Importantly, only molecules with both heavy chains oxidized at Met252 exhibited significantly faster clearance. In contrast, Met428 oxidation had no apparent negative effect on PK and even led to somewhat improved FcRn binding and slower clearance. This minor effect, however, seemed to be abrogated by the dominant effect of Met252 oxidation. The novel approach of functional chromatographic separation of IgG oxidation variants followed by physico-chemical and biological characterization has yielded the first experimentally-backed explanation for the unaltered PK properties of antibody preparations containing relatively high Met252 and Met428 oxidation levels.

## Introduction

The more than 30 approved therapeutic antibodies in clinical use and ~350 in clinical development demonstrate the importance of monoclonal antibodies as therapeutic entities in numerous disease indications, such as oncology, inflammation,

transplantation, infection and ophthalmology.<sup>1,2</sup> Immunoglobulin G (IgG) is the class and format most widely adopted for therapeutic antibodies.<sup>3</sup> The two variable antigen-binding fragments (Fab) of IgG mediate its specificity for the target antigen, while the crystallizable fragment (Fc) is responsible for its effector functions via interaction with the Fcγ receptor (FcγR) family, and

© Jan Stracke, Thomas Emrich, Petra Rueger, Tilman Schlothauer, Lothar Kling, Alexander Knaupp, Hubert Hertenberger, Andreas Wolfert, Christian Spick, Wilma Lau, Georg Drabner, Ulrike Reiff, Hans Koll, and Apollon Papadimitriou

\*Correspondence to: Jan Olaf Stracke; Email: Jan\_olaf.stracke@roche.com

Submitted: 05/07/2014; Revised: 06/14/2014; Accepted: 06/16/2014

<http://dx.doi.org/10.4161/mabs.29601>

This is an Open Access article distributed under the terms of the Creative Commons Attribution-Non-Commercial License (<http://creativecommons.org/licenses/by-nc/3.0/>), which permits unrestricted non-commercial use, distribution, and reproduction in any medium, provided the original work is properly cited. The moral rights of the named author(s) have been asserted.

for its long serum half-life via interaction with the neonatal Fc receptor (FcRn).<sup>4,5</sup>

Maintaining the chemical and structural integrity of antibody therapeutics during manufacturing and shelf-life is a major challenge during pharmaceutical development.<sup>6</sup> In particular, the effect of chemical modifications in the Fc of therapeutic IgGs on FcRn-mediated pharmacokinetic (PK) properties has become the subject of increasing interest for pharmaceutical companies and scrutiny by health authorities. One of the most widely observed and discussed chemical degradation events in IgGs is the oxidation of methionine (Met) to methionine sulfoxide in two positions in the Fc, and understanding its effect on FcRn interaction and PK is crucial to antibody therapeutics development.<sup>7-9</sup> In contrast to other chemical degradation pathways, the activation energy of methionine oxidation is rather low, which explains the focus on its role as one of the main potential causes of protein degradation during refrigerated storage.<sup>10,11</sup>

When investigating the potential effect of chemical modifications on PK properties *in vitro*, analysis of the FcRn/IgG interaction is of vital importance. FcRn is a heterodimeric receptor consisting of two polypeptides, a 48–52 kDa class I major histocompatibility complex-like protein ( $\alpha$ -FcRn) and a 14 kDa  $\beta$ 2-microglobulin ( $\beta$ 2 min). The FcRn/IgG interaction occurs in a strictly pH-dependent manner in the endosomes of vascular endothelial cells and bone marrow-derived cells and functions to salvage IgG from lysosomal degradation.<sup>5</sup> FcRn binds to the CH2-CH3 portion of the Fc domain of IgG with high affinity at acidic endosomal pH.<sup>12,13</sup> The receptor then facilitates the recycling of IgGs to the cell surface and the subsequent release into the blood stream upon exposure of the FcRn/IgG complex to the neutral extracellular pH environment.<sup>14</sup> Crystal structure data and *in vitro* binding experiments indicate that the receptor-antibody interaction can occur in 2:1 stoichiometry, with two FcRn molecules binding to the two heavy chains (HC) of an IgG.<sup>12,15</sup> However, this hypothesis remains to be confirmed *in vivo*.

The FcRn binding region in the CH2-CH3 interface of the Fc contains two methionine residues located at positions 252 in the CH2 domain and 428 in the CH3 domain (Eu numbering<sup>16</sup>), which are highly conserved among IgG isotypes.<sup>17</sup> Both residues are surface exposed, structurally close to the FcRn-binding interface and susceptible to oxidation, with the oxidation rate of Met252 being approximately twice that of Met428.<sup>7,9</sup> A third Met residue at position 358 has been described in some IgG1 alleles and is present in all other IgG subclasses.<sup>17</sup> Its buried location in the CH3 domain at the CH3/CH3 interface between the two antibody HCs and its significant distance to the FcRn binding site renders the oxidation of Met358, and an effect on FcRn binding, unlikely. Most probably due to its structural position, Met358 is found to oxidize at a much slower rate compared with Met252 and Met428 if present.<sup>7,18</sup>

It has been described that Met252 and Met428 oxidation is accompanied by conformational changes in the backbone between residues 242–252 (Eu numbering<sup>16</sup>) of the FcRn binding region.<sup>19-21</sup> Analysis of a truncated antibody Fc demonstrated that the main structural changes upon oxidation occur in the CH2 domain whereas the CH3 is less compromised.<sup>22</sup> Oxidation

of Met252 and Met428 was shown to impair affinity to FcRn and PK properties of monoclonal antibodies.<sup>7-9</sup> However, only IgG preparations with high oxidation levels (~80% oxMet252) exhibited significantly faster clearance compared with non-degraded batches.<sup>8</sup> As a consequence, it has been hypothesized that only molecules with both HCs oxidized at least in one position have markedly altered FcRn affinity and faster clearance *in vivo*.<sup>8,23</sup>

During processing and storage of antibody preparations, oxidation of Met252 and Met428 occurs in parallel at both positions, albeit with different reaction rates.<sup>9,11,24</sup> Even under tailored oxidation stress conditions, it has not been possible to generate antibody samples selectively oxidized at one position only.<sup>7-9,22,25</sup> With the two methionines present in each HC, four oxidation sites exist in the IgG Fc, giving rise to a total of 10 Fc oxidation variants containing 0 to 4 Met oxidations per molecule (Fig. 1).<sup>8</sup> This heterogeneity is the main reason for the current lack of understanding of the contribution of Met252 vs. Met428 oxidation to structural changes, FcRn binding affinity and *in vivo* clearance. Improved understanding of the FcRn affinities and PK properties of these 10 Fc methionine oxidation variants would be of considerable value for the development of antibody therapeutics. The prerequisite for this, however, is the ability to resolve and separate the oxidation variants in a preparative manner for *in vitro* and *in vivo* characterization. So far, attempts using common chromatographic purification techniques have not delivered samples enriched in certain IgG oxidation variants, but rather provided mixtures of antibody species oxidized at both positions, Met252 and Met428.<sup>8,9</sup> Furthermore, site-specific mutations of these two residues can have varying effect on FcRn binding, depending on the nature and size of the introduced amino acid. Mutation of Met252 can significantly increase or decrease the affinity to FcRn, whereas changing Met428 to another amino acid led to stronger affinity to the receptor and prolonged serum half-life *in vivo*.<sup>26</sup> Thus, mutant IgG models to study the consequences of Fc methionine oxidation need to be considered carefully.

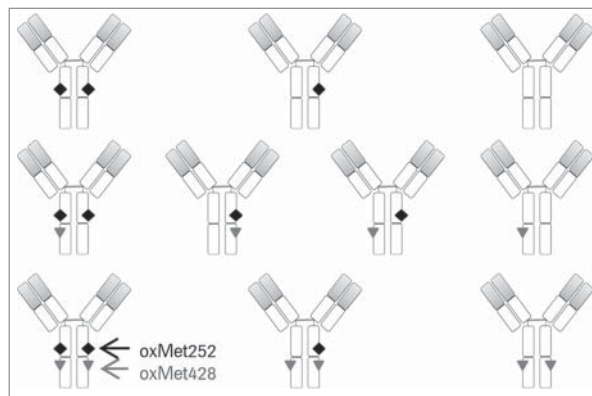


**Figure 1.** Schematic illustration of all 10 IgG Fc methionine oxidation variants. The black diamond represents oxMet252 and the gray triangle indicates oxMet428. The variable domains of HC and LC are shaded in gray.

In the study presented here, we applied a novel pH-gradient FcRn affinity chromatography method that closely mimics the physiological conditions of interaction between FcRn and IgG to isolate three functionally distinct antibody oxidation variants from a hydrogen peroxide-treated IgG1 batch based on their different FcRn-binding properties.<sup>27</sup> The structure-function relationship of Fc methionine oxidation could be established, and the individual contribution of oxMet252 vs. oxMet428 to FcRn affinity loss and PK impairments could be clarified.

Our results provide the first experimentally-backed explanation for the observation that even antibody preparations with relatively high total Fc methionine oxidation levels (e.g., 40% oxMet252 and 25% oxMet428) do not show markedly impaired PK profiles. The effect of Fc methionine oxidation on antibody PK and functionality may be re-assessed for future pharmaceutical development on the basis of this study.

## Results

### FcRn affinity chromatography of H<sub>2</sub>O<sub>2</sub>-treated mAb1 and isolation of 3 main oxidation variants

We recently developed an analytical pH gradient FcRn affinity liquid chromatography method with conditions closely resembling the physiological mechanism of interaction between IgGs and FcRn.<sup>27</sup> In the current study, using a refined pH-gradient, FcRn chromatography analysis of monoclonal IgG1 and IgG4 preparations reproducibly yielded one single peak as shown for the representative IgG1 mAb1 (Fig. 2, black curve). After hydrogen peroxide treatment, the chromatogram of the antibody, now termed mAb1\_Ox, exhibited three distinct peaks, whereby the retention time of the last eluting peak corresponds to the main peak in the untreated mAb1 sample (Fig. 2, gray curves). Two additional peaks, named prepeaks I and II, eluted earlier and at

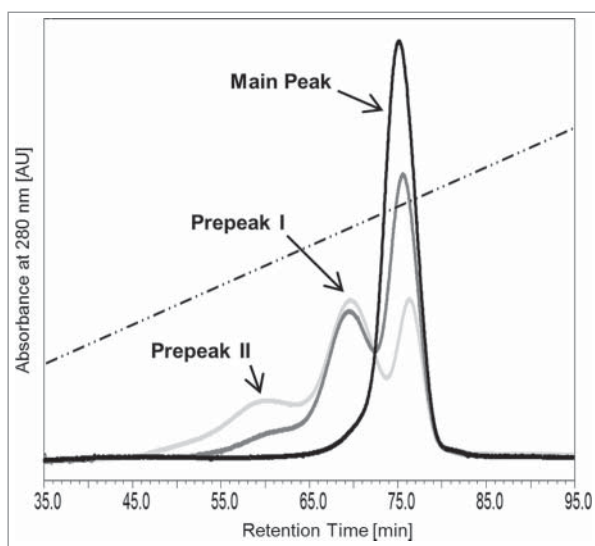


**Figure 2.** Analytical FcRn affinity chromatography of mAb1 (black curve) and H<sub>2</sub>O<sub>2</sub>-treated mAb1\_Ox (0.01 and 0.02% v/v, dark gray and light gray curves, respectively). The dotted line indicates the pH gradient.

lower pH in the gradient than the main peak. Thus, the FcRn column resolved a total of 3 distinct antibody oxidation variants in the hydrogen peroxide-treated sample mAb1\_Ox that differed in their affinity to FcRn, with the latest eluting variant (main peak) exhibiting the highest and the earliest eluting variant (prepeak II) the lowest FcRn binding properties.

In order to characterize and compare the 3 resolved oxidation variants with regard to their physico-chemical, functional and PK properties, a preparative version of the FcRn affinity column was established. Approx. 200 mg of mAb1, that exhibit only a single main peak eluting at ~82 min, were treated with 0.01% (v/v) hydrogen peroxide for 18 h (Fig. 3A and B). This oxidized material mAb1\_Ox, exhibiting 3 peaks, was applied to the preparative FcRn affinity column and 10 mg of each peak were isolated for further in vitro and in vivo characterization (Fig. 3C). Because the three peaks were not base-line resolved, the peak valleys were not included in the fraction pools in order to obtain the individual variants as pure as possible (Fig. 3C). The 3 fraction pools, original mAb1 and mAb1\_Ox were dialyzed in formulation buffer containing 5 mM L-methionine to suppress further oxidation. The protein concentration was adjusted to 1 mg/ml in all samples and aliquots were stored frozen below -60 °C to avoid any further degradation and modification.

After the described separation and preparation, five samples were obtained for characterization: (1) the untreated antibody mAb1; (2) a portion of the same antibody batch that was treated with hydrogen peroxide, mAb1\_Ox; (3) the 3 peaks isolated from mAb1\_Ox using the FcRn column, mAb1\_Ox\_main peak; (4) mAb1\_Ox\_prepeak I; and (5) mAb1\_Ox\_prepeak II (Fig. 3).

### Characterization of isolated mAb1 oxidation variants

To verify the successful isolation of the three antibody oxidation variants from mAb1\_Ox, the samples were subjected to analytical FcRn chromatography and compared with the starting material (mAb1) and the H<sub>2</sub>O<sub>2</sub>-treated, non-fractionated batch (mAb1\_Ox) (Fig. 4). The results demonstrated that the three peaks were purified without detectable contaminations of the respective neighboring species. Subsequently, all five samples were extensively characterized with regard to their quality, assessing the following analytical parameters: Color, turbidity, aggregation and fragmentation (SE-HPLC, CE-SDS red./non-red.), charge heterogeneity (CE-IEF, cIEX), oligosaccharide pattern (RP-UPLC of 2AB-labeled glycans), endotoxin content (LAL gel clotting assay), target binding (SPR target binding assay; Biacore), and functionality (molecule-specific qualified cell-based assay). The results generated using these analytical methods unanimously demonstrated that all five samples were of high product quality and not significantly different with regard to purity, integrity and functionality (data not shown).

To determine potential differences in the nature and quantity of chemical modifications, all samples were subjected to tryptic LC-MS peptide mapping. The four samples that encountered hydrogen peroxide treatment (mAb1\_Ox\_...) exhibited low levels of methionine and tryptophan oxidation in the complementarity-determining regions that, however, did not affect target

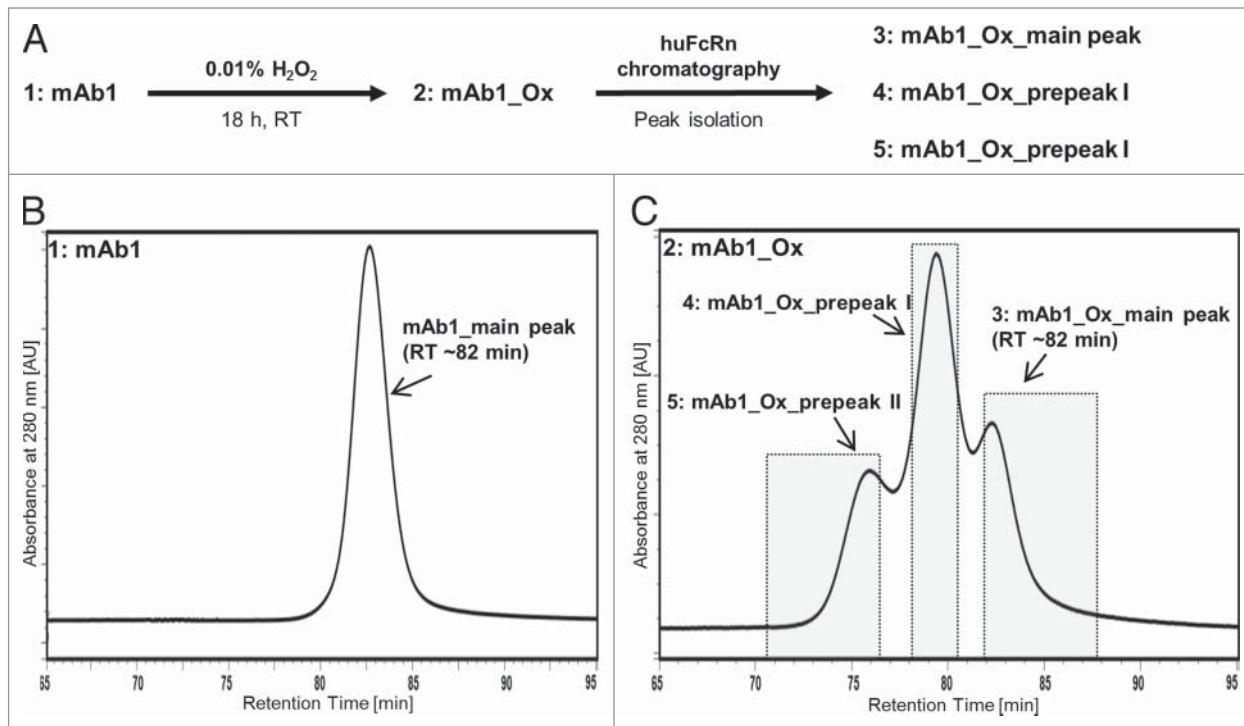


**Figure 3.** (A) Schematic illustration of sample preparation of five mAb1-derived samples for further characterization. (B) FcRn chromatogram of untreated mAb1. (C) FcRn chromatogram of mAb1\_Ox; the three separated peaks were individually collected and pooled as indicated by the gray rectangles.

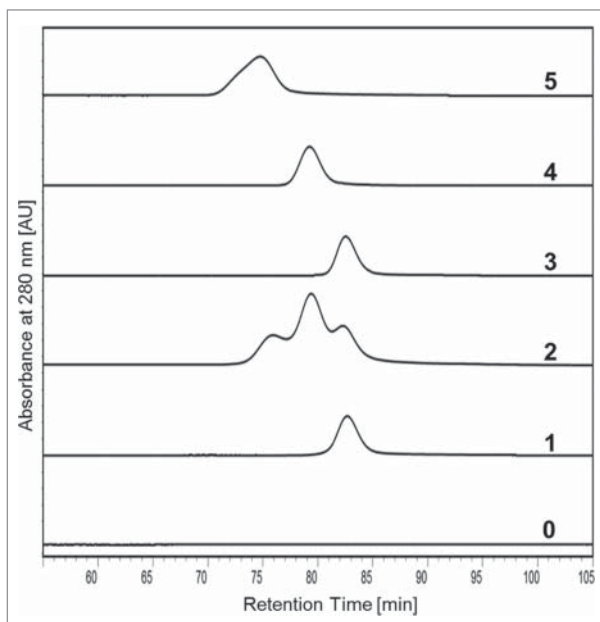


**Figure 4.** Overlay of the analytical FcRn chromatograms of the five mAb1-derived samples in comparison to placebo buffer. (0) Placebo, (1) mAb1, (2) mAb1\_Ox, (3) mAb1\_Ox\_main peak, (4) mAb1\_Ox\_prepeak I, (5) mAb1\_Ox\_prepeak II.

binding and in vitro functionality (data not shown). Due to their distance from the FcRn binding region, and since no effect was observed on target binding, these oxidations were not considered relevant for FcRn-dependent functionality. The only significant differences that could be detected among the five samples were considerable variations in the overall content and ratio of oxidized Fc methionines, oxMet252 and oxMet428.

As expected, untreated antibody mAb1 exhibited base-line oxidation levels, with 5% oxMet252 and 2% oxMet428. In contrast, the unfractionated hydrogen peroxide-treated mAb1\_Ox contained considerably higher oxidation levels, with 41% of Met252 and 28% of Met428 residues affected (Table 1). Surprisingly, a very strong and stepwise increase of oxMet252 from 3 to 50 to 90% was detected in mAb1\_Ox\_main peak, mAb1\_Ox\_prepeak I and mAb1\_Ox\_prepeak II, respectively. These increasing oxMet252 levels clearly correlate with the stepwise decrease in retention time and affinity on the FcRn column (Fig. 4; Table 1). In contrast, oxidation levels at position Met428 showed no strict correlation with retention time and affinity on the column. They differed insignificantly between mAb1\_Ox\_main peak (20% oxMet428) and mAb1\_Ox\_prepeak I (23% oxMet428) and were only increased to 42% in mAb1\_Ox\_prepeak II. These results strongly suggest that oxidation of Met252, but not of Met428, has a dominant negative effect on FcRn affinity.

The theoretical FcRn:IgG binding stoichiometry is 2:1, with one FcRn molecule binding to each of the two IgG HCs.<sup>15,28</sup> In

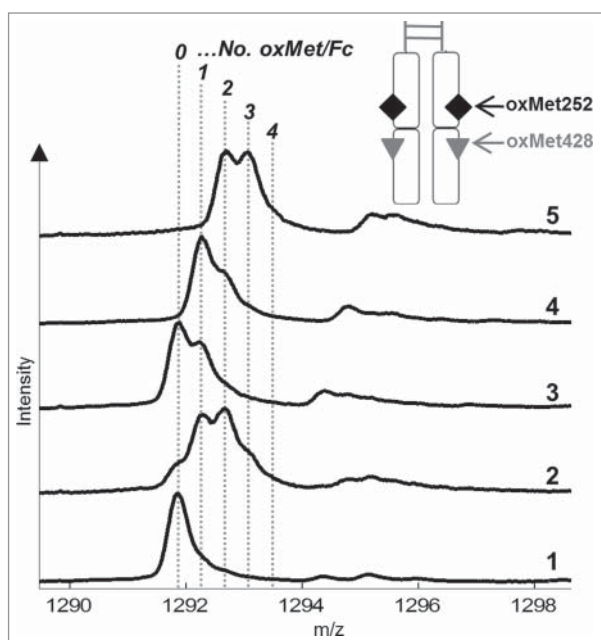


**Figure 5.** ESI-MS analysis results of plasmin-digested samples: (1) mAb1, (2) mAb1\_Ox, (3) mAb1\_Ox\_main peak, (4) mAb1\_Ox\_prepeak I, (5) mAb1\_Ox\_prepeak II. Signals in the mass spectra represent number of methionine oxidations (indicated by dotted lines and italic numbers; +16 Da for each oxidation) in the intact Fc (minimum 0, maximum 4 oxMet per Fc). The sketch shows the resulting fragment after plasmin digest: Disulfide-linked, intact Fc with 4 potential oxMets.

addition, in an IgG batch, three molecule variants differing in their Met252 oxidation content can exist, Met252/Met252, oxMet252/Met252, and oxMet252/oxMet252. Here, the observed steep and stepwise FcRn affinity reduction of the three isolated species from mAb1\_Ox is accompanied by the equally stepwise increase in oxMet252 content (Fig. 4; Table 1). This strongly suggests that the three peaks isolated from mAb1\_Ox indeed correspond to the 3 Met252 oxidation variants. Accordingly, both HCs of mAb1\_Ox\_main peak are basically unaffected (3% oxMet252), whereas mAb1\_Ox\_prepeak I (50% oxMet252) and mAb1\_Ox\_prepeak II (90% oxMet252) represent antibody species oxMet252/Met252 (one HC oxidized at Met252) and oxMet252/oxMet252 (both HCs oxidized at Met252), respectively.

To verify that the number of oxMet252 per IgG is the main determinant for the distinct pH-dependent FcRn binding properties of the three isolated variants on the column, a plasmin digest followed by LC-ESI-mass spectrometry analysis of all five samples was performed (Fig. 5). Since plasmin cleaves the HCs specifically between lysine and threonine N-terminal of the hinge double-disulfide bonds (S[219]-C-D-K-T-H-T-C-P-P-C-P-A-P-E-L-L-G-G-P(238)), this treatment generates Fc with intact covalent linkage between the two Fc HC fragments. After deglycosylation, the resulting Fc of all five samples were analyzed. In contrast to the full-length antibodies, the Fc can be analyzed for oxidation events with greatly improved resolution using mass spectrometry due to their lower molecular mass of ~50 kDa.

Since hydrogen peroxide treatment induced oxidation in the Fc only at positions Met252 and Met428 (methionine sulfoxide, +16 Da) as confirmed by peptide map analysis, the Fc can exhibit a minimum of 0 (neither Met252 nor Met428 oxidized in both HCs) and a maximum of 4 (both HCs oxidized at Met252 and Met428) methionine oxidations in total.

As indicated by a relatively homogeneous signal in the mass spectrum, mAb1 Fc contains predominantly 0 methionine oxidation (0 oxMet) with low levels of single-oxidized Fc (1 oxMet) (Fig. 5). In contrast, the mAb1\_Ox Fc exhibits the most heterogeneous mass spectrum of all five samples with a mixture of all oxidation variants from 0 to 4 oxMet. The Fc of mAb1\_Ox\_main peak and mAb1\_Ox\_prepeak II contain predominantly 0 to 2 and 2 to 4 oxMet, respectively, whereas the intermediate fraction mAb1\_Ox\_prepeak I exhibits 1 to 3 oxMet in its Fc. In agreement with the peptide map data and the FcRn affinity column elution profile, these results complete the picture of the oxMet252 vs. oxMet428 distribution in the 3 isolated mAb1\_Ox oxidation variants (Fig. 6; Table 1).

In summary, mAb1\_Ox\_main peak contains antibody variants that are predominantly oxidized at position Met428, but not at Met252. The plasmin digest indicates that the 20% oxMet428 found in this fraction are most probably distributed statistically. Apart from the dominant 0 oxMet signal, a significant 1 oxMet and a smaller 2 oxMet signal can be detected in the mass spectrum (Fig. 5). In analogy, mAb1\_Ox\_prepeak II contains predominantly antibody variants that carry oxMet252 in both HCs (90% oxMet252 in total). This is confirmed by the detection of a minimum of 2 oxMet in the corresponding mass spectrum of the plasmin digested sample. The 42% of Met428 in this sample are most probably also distributed statistically due to the presence of a significant 3 oxMet signal and a less prominent 4 oxMet signal in the mass spectrum of the Fc. The intermediate fraction, mAb1\_Ox\_prepeak I Fc (50% oxMet252) exhibits a minimum of one oxidation (1 oxMet) in addition to a significant quantity of 2 oxMet and lower levels of 3 oxMet. The complete absence of 0 and 4 oxMet in this fraction, which would have been present if both, oxMet252 and oxMet428, were distributed statistically, demonstrate that all antibody variants in mAb1\_Ox\_prepeak I carry at least one oxMet252. Hence, the hypothesis that the affinity of mAb1 oxidation variants to FcRn in the pH-gradient of the FcRn chromatography predominantly depends on the total number of Met252 oxidations per antibody molecule—0, 1, or 2 oxMet252—but not on the oxidation status at position Met428, has been verified by the accumulated analytical data. The results of these analyses are summarized in Table 1 and Figure 6 with the 10 IgG oxidation variants assigned to the corresponding peaks in the FcRn chromatogram.

To complement these data that strongly suggest that Met252 oxidation is the dominant negative factor for FcRn/IgG interactions, a second *in vitro* FcRn-binding assay on SPR basis and an *in vivo* evaluation in a relevant PK model was performed with the five samples.

#### FcRn binding analysis

Surface plasmon resonance (SPR) analysis was performed to characterize the properties of the five samples with regard to FcRn

**Table 1.** Summary of sample characterization results

Sample	Peptide Map		Plasmin digest/ ESI-MS
	oxMet252 [%]	oxMet428 [%]	No. oxMet per Fc
1: mAb1	5	2	0, 1
2: mAb1_Ox	41	28	0, 1, 2, 3, 4
3: mAb1_Ox_main peak	3	20	0, 1, 2
4: mAb1_Ox_prepeak I	50	23	1, 2, 3
5: mAb1_Ox_prepeak II	90	42	2, 3, 4

Note: Left column: Sample names. Middle column: Total oxMet252 and ox Met428 levels from tryptic LC-MS peptide map analysis. Right column: Numbers of oxMet per Fc (minimum 0, maximum 4 oxMet) from LC-ESI-MS analysis of plasmin-digested samples.

binding. For this, the nature of the on-rate, the total binding levels (RU max.) and the characteristics of the dissociation were assessed (Fig. 7A and B). MAb1\_Ox exhibited a significant decrease of 21% in total binding levels compared with mAb1. After fractionation, mAb1\_Ox\_main peak showed the highest overall binding and slowest off-rate of all five samples with the 6% improvement in total binding compared with mAb1 being significant. The binding properties of this variant are noteworthy considering the 20% oxMet428 (and 3% oxMet252) content of mAb1\_Ox\_main peak

compared with baseline oxidation levels in mAb1 (Table 1). These data suggest that oxMet428 does not impair the FcRn/IgG interactions and may even hint toward a positive effect on FcRn affinity. In comparison to mAb1 and mAb1\_Ox\_main peak, mAb1\_Ox\_prepeaks I and II show a significant and stepwise loss of binding levels and increased off-rates. The RU max. values of mAb1\_Ox\_prepeak I and mAb1\_Ox\_prepeak II are reduced by 33% and 67%, respectively, compared with mAb1. In summary, data from SPR-based FcRn binding analysis nicely correlated with the binding properties of the five samples observed on the FcRn affinity column (Figs. 4 and 7).

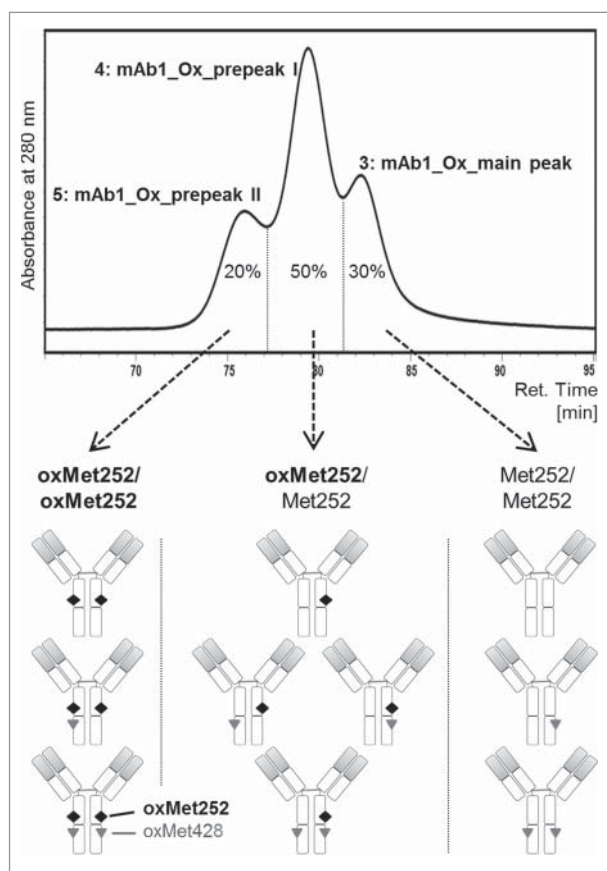


**Figure 6.** FcRn chromatogram of mAb1\_Ox with the relative peak areas of the 3 separated peaks. Arrows indicate the mAb1 oxidation variants in the 3 peaks according to the results of LC-MS peptide map and plasmin digest/ESI-MS analysis.

#### PK in human FcRn-transgenic mice

The stepwise reduction of FcRn affinity of the three isolated mAb1 oxidation variants demonstrated by FcRn chromatography and SPR analysis suggested an impact on in vivo clearance due to impairment of the FcRn-mediated IgG recycling mechanism. To explore the effect of Met252 and Met428 oxidation on antibody clearance and terminal half-life, a PK study was performed in a human FcRn-transgenic mouse model. HuFcRn-transgenic mice were chosen to provide for the well-known species-specificity of the FcRn/IgG interaction.<sup>29</sup> Importantly, mAb1 does not bind to the murine target. HuFcRn transgenic mice were injected intravenously with a single dose of the five samples at a dose level of 10 mg/kg. The corresponding serum concentrations were analyzed over a time period of 28 d. Serum concentrations vs. time profiles of all samples exhibited a biphasic profile with an initial rapid decrease in antibody serum concentration within the first 24 h followed by a log-linear decline over time as shown in Figure 8A. PK parameters calculated from these curves revealed that only mAb1\_Ox\_prepeak II had a significantly higher systemic clearance rate of  $0.083 \pm 0.008$  mL/min/kg compared with untreated mAb1 ( $0.044 \pm 0.002$  mL/min/kg;  $P < 0.0001$ ). MAb1\_Ox and mAb1\_Ox\_prepeak I, showed apparent faster systemic clearance rates of  $0.048 \pm 0.003$  and  $0.049 \pm 0.002$  mL/min/kg, respectively (Fig. 8B). However, these values are not significantly different compared with the ones obtained for mAb1 ( $P$  values  $\geq 0.059$ ).

Interestingly, mAb1\_Ox\_main peak is cleared significantly slower compared with the non-oxidized mAb1 control sample ( $0.038 \pm 0.002$  mL/min/kg;  $P = 0.022$ ). Although this difference is rather small and at the limit of significance, it is in agreement with the FcRn SPR analysis data obtained for this sample

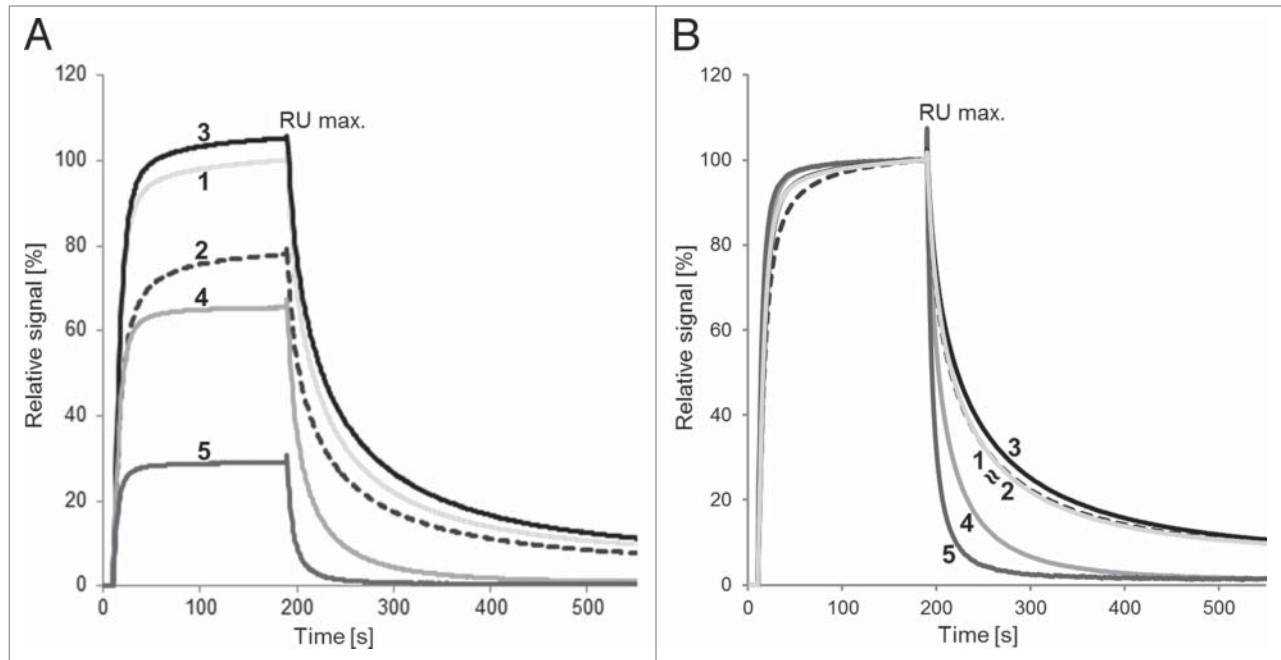


**Figure 7.** SPR analysis of FcRn/IgG interaction. **(A)** Binding level (on-rate). **(B)** Off-rates (normalized RU max. values). Samples: (1) mAb1, (2) mAb1\_Ox, (3) mAb1\_Ox\_main peak, (4) mAb1\_Ox\_prepeak I, (5) mAb1\_Ox\_prepeak II. Evaluation of SPR-data was performed by comparison of the biological response signal height at 180 s after injection. All signals were normalized to mAb1 (100%).

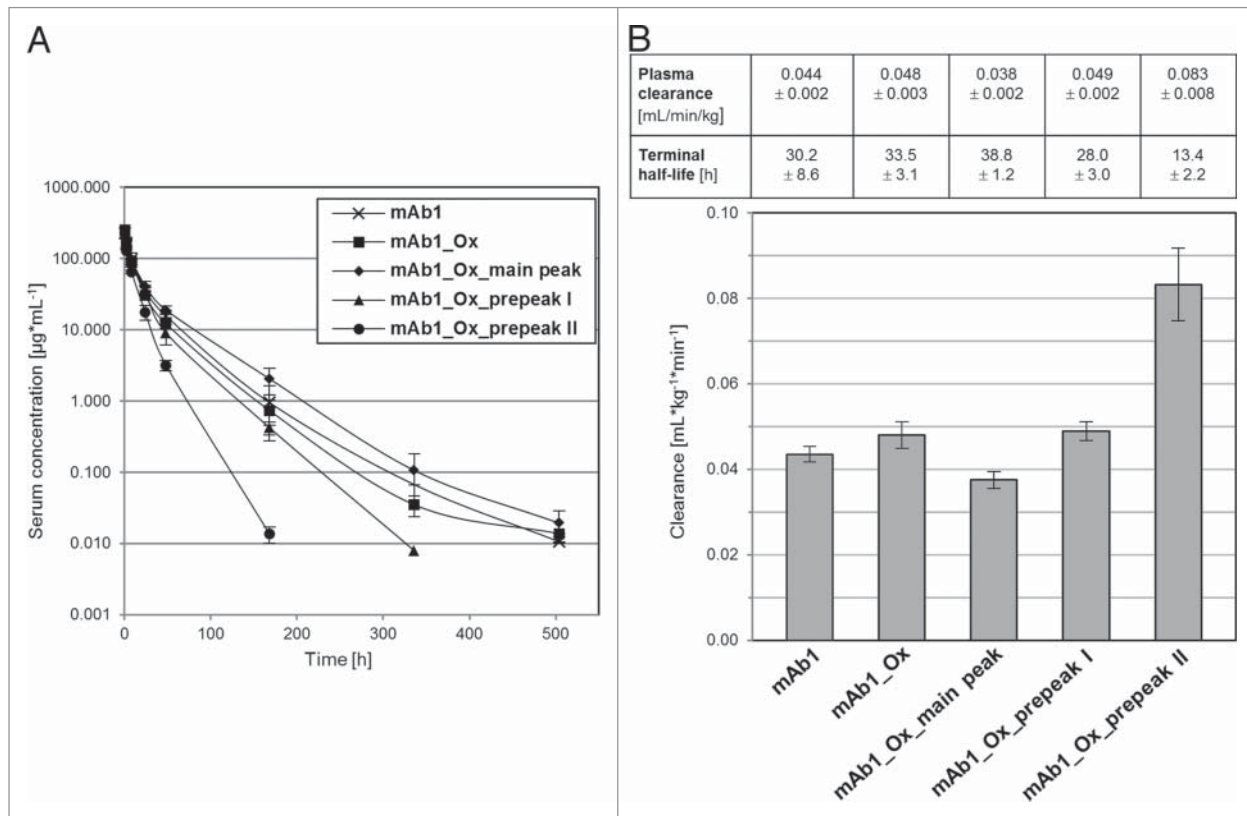


**Figure 8.** Pharmacokinetic analysis in huFcRn-transgenic mice. **(A)** Serum concentration over time after single bolus injection. Samples: (1) mAb1, (2) mAb1\_Ox, (3) mAb1\_Ox\_main peak, (4) mAb1\_Ox\_prepeak I, (5) mAb1\_Ox\_prepeak II. **(B)** Bar diagram of plasma clearance. Corresponding clearance and terminal half-life values for all 5 indicated samples are given in the table above the graph.

and suggests that the 20% oxMet428 content may result in improved FcRn affinity and PK properties.

Direct comparison of the PK parameters of the three isolated mAb1\_Ox fractions mAb1\_Ox\_mainpeak, mAb1\_Ox\_prepeak I and mAb1\_Ox\_prepeak II revealed a stepwise increase in clearance that is in accordance with the sequential FcRn chromatography elution profile and the stepwise decrease of total binding levels in SPR analysis. Using a Pearson correlation test, it was demonstrated that the systemic clearances of the three antibody oxidation variants were significantly different from each other ( $P$  values  $< 0.0001$ ).

Serum terminal half-life values were 2.3-fold lower for mAb1\_Ox\_prepeak II ( $t_{1/2} = 13.4 \pm 2.2$  h) compared with its untreated control mAb1 ( $t_{1/2} = 30.2 \pm 8.6$  h) (Fig. 8B). Terminal half-lives of the three purified variants decreased stepwise from  $38.8 \pm 1.2$  h (mAb1\_Ox\_main peak) to  $28.0 \pm 3.0$  h (mAb1\_Ox\_prepeak I) to  $13.4 \pm 2.2$  h (mAb1\_Ox\_pre peak II), and therefore are inversely correlated with increasing levels of Met252 oxidation. mAb1\_Ox\_main peak, despite carrying 20% oxMet428, showed the longest terminal half-lives ( $t_{1/2} = 38.8 \pm 1.2$  h) among all compounds tested ( $P \leq 0.0216$ ) and compared with untreated mAb1.

## Discussion

### Structure-function relationship—current situation

The detailed understanding of the structure-function relationship of Fc methionine oxidation is of great importance for the development of therapeutic antibodies. The limited knowledge of how exactly Met252 and Met428 oxidation influence the PK of therapeutic IgGs necessitates considerable efforts to monitor these modifications upon release and storage of drug substance and drug product batches. Fc methionine oxidation is generally regarded as a potential critical quality attribute (pCQA) and changes in the Met oxidation levels during manufacturing or storage raise justified questions concerning the effect on shelf-life and in vivo clearance.

In previous studies, oxidized antibody batches were evaluated that differed in their total Met oxidation levels, but always contained both oxMet252 and oxMet428, with the former being more prominent.<sup>8,9,22</sup> As the four methionine residues in an IgG Fc give rise to a total of 10 oxidation variants (Fig. 1) with potentially distinct FcRn affinities and PK profiles, it is not feasible using such mixtures to investigate which variants are altered in their properties and which are not.<sup>8</sup> This is complicated by the fact that an antibody can theoretically be bound by two FcRn molecules, one per HC.<sup>35</sup> Therefore, methionine oxidation in only one HC of an IgG, even at both positions, may not result in faster clearance since the other HC is still able to fully interact with FcRn. This clearly highlights the demand for a different approach to investigate the effect of Fc methionine oxidation on FcRn binding and PK in more detail.

Available chromatographic methods, such as Protein A affinity chromatography, are valuable analytical tools to resolve and assess overall Fc methionine oxidation levels in degraded antibody

samples, but they are not capable of separating functionally distinct oxidation variants with sufficient resolution.<sup>8,9,21,32</sup>

Attempts to oxidize one methionine position selectively while leaving the second position intact have all failed, since both positions are similarly prone to oxidation. The rate of oxidation of Met252 is approximately twice that of Met428, leading to a higher oxMet252 than oxMet428 content after forced oxidation or real-time storage.<sup>7-9,22,25</sup> The use of point mutations to mimic or block oxidation either at Met252 or Met428 leads to considerable changes in the affinity to FcRn, likely due to structural distortions in the Fc.<sup>26,33</sup> Exchange of Met252 and Met428 has been shown to compromise or increase FcRn interactions.<sup>26,34</sup> Such mutational approaches are of value, but cannot simulate the situation of methionine oxidation exactly. They need to be designed with great care in order to enable conclusions relevant for the wild-type situation. Due to these reasons, a highly resolved structure-function relationship of the individual effect of oxMet252 and oxMet428 has not been established yet.

### Relevance of pH gradient FcRn chromatography

The pH gradient FcRn affinity chromatography method used in this study was recently introduced as a new analytical tool for monitoring the interactions of monoclonal antibodies and FcRn in vitro under physiological conditions.<sup>27</sup> In contrast to other analytical methods commonly applied to study FcRn/IgG interactions in vitro (e.g., SPR), FcRn affinity chromatography conditions reflect the pH-dependency of the interaction in an unprecedented manner.<sup>13</sup> While SPR analysis only yields overall kinetic or binding values and is unable to resolve and quantify antibody species differing in their affinity to the receptor, FcRn affinity chromatography allows direct identification and quantification of individual IgG species with altered binding functionalities. Adjustment of the pH gradient allows optimal separation and characterization of antibody variants detected in a sample of interest. In comparison to common chromatographic methods (e.g., size exclusion or ion-exchange chromatography) that utilize artificial matrices and binding groups for separation, FcRn chromatography resolves molecule species based on their affinity to an immobilized physiological interaction partner.<sup>21,30,31</sup> Similar to these methods, FcRn chromatography can be scaled up to facilitate preparative isolation of variants. This enables secondary characterization strategies for the separated variants, such as physico-chemical analysis and PK assessment, and facilitates the establishment of structure-function relationships.

### Effect of methionine oxidation on FcRn binding

The monoclonal therapeutic antibody mAb1 used for this investigation is a representative IgG1 kappa. MAb1 and numerous other therapeutic antibodies, IgG1 and IgG4, have all exhibited the same peak pattern on the FcRn affinity column after hydrogen peroxide treatment or storage under accelerated conditions. Therefore, mAb1 is considered a representative model to study the structure-function relationship and the consequences of Fc methionine oxidation on FcRn-dependent PK of therapeutic antibodies in general.



After chromatographic isolation of the three peaks from mAb1\_Ox, extended physico-chemical characterization of the fractionated peaks and two control samples revealed no significant differences in purity, integrity and target binding. Indeed, the only significant modifications that differed strongly among the five samples were the quantity and distribution of Met252 and Met428 oxidations in the Fc.

The stepwise increase of oxMet252 levels in the three isolated peaks correlated well with a decrease in retention time on the FcRn column and faster off-rates in the SPR analysis, whereas oxMet428 levels did not show a similar correlation. The oxMet252 increase in the three peaks corresponds to the number of oxMet252 per IgG: 0, 1, or 2.

Our results strongly suggest that oxidation of Met252, but not, or to a significantly lesser extent, of Met428, results in functional alterations of the FcRn binding properties of antibodies. Wang et al.<sup>21</sup> have previously indicated that oxidation of Met252 (CH2 domain) and Met428 (CH3 domain) is accompanied by subtle conformational changes in the FcRn binding region. Studies using a truncated antibody Fc demonstrated that the main structural changes upon oxidation occur in the CH2 domain, whereas the CH3 is less compromised.<sup>22</sup> The melting temperature ( $T_m$ ) of the CH2 domain is markedly decreased upon oxidation while the  $T_m$  of the CH3 only changes slightly. In support of these findings, the rates of deamidation of two CH2 asparagine residues were significantly increased upon oxidation, while those of other residues were not affected. These results are in excellent agreement with our melting temperature data of an oxidized full-length IgG1 (data not shown). The regions undergoing significant structural changes by oxidation of Met252 and Met428 were mapped to CH2 residues 243–247 using hydrogen/deuterium exchange LC-MS peptide mapping.<sup>20</sup> In the same report, a detailed molecular mechanism for the affinity reduction between FcRn and IgG induced by Met252 oxidation has been suggested. Impaired hydrophobic interactions between oxMet252 and Pro134 of FcRn and repulsion between oxMet252 and Glu135 seem to be responsible for the decrease in affinity. While Met252 oxidation directly affected FcRn/IgG binding, Met428 oxidation is hypothesized to destabilize the CH2-CH3 hinge region, probably by disrupting the hydrophobic core formed between CH2 and CH3.<sup>20</sup> However, our results and the data reported by Hinton et al.<sup>26</sup> on Met428 oxidation and site-specific mutants, respectively, may suggest that molecular changes at this position may also lead to improved FcRn binding.

#### Pharmacokinetic characterization—effect of oxMet252 vs. oxMet428

The relevance of the FcRn chromatography and SPR results was corroborated by the results of the PK experiments in mice transgenic for human FcRn. This model is extremely valuable, and the only non-primate surrogate system available to study FcRn-mediated PK properties of therapeutic antibodies and antibody variants in vivo. Its predictive value for the primate situation has been demonstrated previously by analyzing PK

properties of IgG Fc variants in monkeys.<sup>27,36,37</sup> These reports suggest that the observed consequences of methionine oxidation should be translatable to the monkey and human system.

The PK data of the five samples compellingly demonstrated for the first time for a wild-type IgG1 that oxidation of Met252, but not, or to a much lesser extent, of Met428, has a negative impact on FcRn-mediated PK properties. The significant differences in plasma clearance rates between the three isolated FcRn chromatography peaks strongly support the hypothesis that FcRn can interact with antibodies in vivo in a 2:1 stoichiometry.

Importantly, compared with the untreated mAb1 sample, only the oxMet252/oxMet252 species (mAb1\_Ox\_pre-peak II), but neither Met252/oxMet252 (mAb1\_Ox\_pre-peak I) nor Met252/Met252 (mAb1\_Ox\_main peak) species, were cleared significantly faster.

The similar PK profile of mAb1\_Ox\_prepeak I (Met252/oxMet252) and mAb1 (Met252/Met252) strongly suggests that the interaction of a single functional HC with FcRn is enough to convey the typical antibody PK. According to these findings, a 1:1 stoichiometry for the FcRn/IgG1 interaction is sufficient in vivo. However, the ~20% difference in the Met428 oxidation content between these two samples also has to be considered. Interestingly, antibody species with only increased Met428 oxidation levels (mAb1\_Ox\_main peak: 20% oxMet428), but baseline oxMet252 content (3%), exhibited increased affinity to FcRn in SPR analysis and significantly slower plasma clearance compared with mAb1 control. These surprising results, which may suggest a positive effect of Met428 oxidation on FcRn binding and PK, are in agreement with previous studies in which Met428Leu mutants were evaluated in rhesus monkeys.<sup>26</sup> This mutant showed an 11-fold increase in binding to human FcRn at pH 6.0 compared with the wild-type counterpart in a competitive FcRn binding assay. PK analysis in rhesus monkeys demonstrated an ~2.3-fold lower mean clearance for a T250Q/M428L double mutant compared with wild-type IgG.<sup>26</sup> While the dominant negative impact of Met252 oxidation on FcRn/IgG interactions and in vivo clearance is apparent from our results, the potential positive effect of Met428 oxidation is less evident, but should at least be considered for data interpretation.

The substantial levels of Met252 (41%) and Met428 (28%) oxidation make it difficult to comprehend why mAb1\_Ox showed a similar PK profile as mAb1. However, coinciding observations have been reported previously by Wang et al.<sup>8</sup> and may be explained by interpretation of our data. mAb1\_Ox is comprised of a mixture of three main mAb1 oxidation variants with each showing a distinctive PK profile in our study. The integration of the relative peak areas in the analytical FcRn chromatogram of mAb1\_Ox yielded: 30% mAb1\_Ox main peak with the slowest clearance of all five samples (even slower than mAb1), 20% mAb1\_Ox\_prepeak II with the fastest clearance (approx. twice the rate of mAb1), and 50% mAb1\_Ox\_prepeak I with a clearance that is slightly, but not significantly, faster than that of mAb1 (Figs. 6 and 8B). This composition may help to explain the relatively indistinguishable PK profile of mAb1\_Ox compared with mAb1. The fast clearance of 20% of the antibodies (mAb1\_Ox\_prepeak II) in the mixture seems to be partially

compensated by 30% of molecules that exhibit a small, but significantly slower clearance (mAb1\_Ox\_main peak). From the relative quantities of the three variants in mAb1\_Ox, obtained from the integrated peak areas, and from the clearance values of the three isolated variants, a theoretical clearance for mAb1\_Ox can be calculated that corresponds accurately to the plasma clearance experimentally determined in the PK study (data not shown). Thus, the experimental data indeed support the hypothesis that oxidation at Met428 alone may lead to somewhat improved FcRn binding.

If Met428 oxidation actually has this effect, it is surprising that 42% oxMet428 in the mAb1\_Ox\_prepeak II sample were not able to compensate some of the effect of the 90% oxMet252. On the contrary, the clearance of this sample is markedly faster than expected from the clearance slope between mAb1\_Ox\_main peak and prepeak I. It appears that Met428 oxidation can amplify the reduction in FcRn affinity and increase in clearance if it occurs in parallel to Met252 oxidation. Possibly, Met428 oxidation has an additional negative effect on FcRn binding only if co-located on the same HC with oxMet252. In this case, the higher oxMet428 levels in mAb1\_Ox\_prepeak II compared with the other two peaks may be the result of the fractionation procedure. In this sample, the early eluting flank of the peak was included, while it was omitted during fractionation of the two other peaks (Fig. 3C). For example, for mAb1\_Ox\_main peak, only the late eluting 2/3 of the peak were collected. In case there would be a gradient of oxidation sub-species within the three peaks, the variants

containing both oxMet252 and oxMet428 on the same HCs would most probably exhibit the lowest affinity to the FcRn column, and thus elute in the front flank of the respective peaks. This hypothesis can be supported by the asymmetrical shape of mAb1\_Ox\_prepeak II that exhibits a small shoulder at lower retention times (Fig. 3C). Further studies of the distribution of oxMet428 and oxMet252 within the individual three peaks are required to investigate this.

Another potential reason for the higher oxMet428 levels in mAb1\_Ox\_prepeak II is that preceding Met252 oxidation induces structural changes that in turn lead to higher solvent exposure of Met428, and thereby an increased oxidation rate.

In summary, it appears that Met428 oxidation has no significant negative consequence and may even lead to somewhat increased FcRn affinity if not accompanied by Met252 oxidation. On the other hand, it seems to amplify the loss of FcRn affinity and impairment of PK properties when it occurs in parallel (on the same HC) to the faster and functionally dominant Met252 oxidation.

#### Relevance for the analytical control strategy and the in vivo situation

Although the FcRn chromatography method is a valuable analytical tool that allows the separation and quantification of the 3 Met252 oxidation variants based on their FcRn affinity, it is not yet established as a standard release or characterization method for monoclonal antibodies. Overall methionine oxidation is generally quantified using LC-MS peptide map analysis.

Assuming that methionine oxidation occurs under first-order kinetics and that the rate of Met252 oxidation is approx. twice that of Met428 oxidation, it is actually possible to simulate the relative quantities of all 10 oxidation species for a certain IgG lot with known total oxMet252 and oxMet428 levels using a model described previously.<sup>8,23</sup> This model could not be verified experimentally up to now because a method to separate the 10 oxidation variants for quantification and analytical characterization did not exist. Using FcRn affinity chromatography, we could now determine the distribution of the three main Met252 oxidation variants in mAb1\_Ox (Met252/Met252, oxMet252/Met252, and oxMet252/oxMet252) experimentally. Although the column was not capable of fully resolving the additional Met428 oxidation heterogeneity within

mAb1_Ox FcRn Chromatogram	mAb1_Ox_prepeak II (20%)	mAb1_Ox_prepeak I (50%)	mAb1_Ox_main peak (30%)
Met252 oxidation variant <sup>2</sup>	oxMet252/oxMet252	oxMet252/Met252	Met252/Met252
Met252/Met428 oxidation variant			
oxMet252 ◆ oxMet428 ▼			
Simulation [%] <sup>3</sup>	1    6    10	2    8    8    30	2    12    21
Experiment [%] <sup>4</sup>	3    10    7	2    9    9    30	1    10    19
Clearance compared to mAb1	2-fold faster	similar	similar to slightly slower

**Scheme 1.** Relative distribution of all 10 mAb1 methionine oxidation variants in mAb1\_Ox. Due to the homodimeric structure of IgG, the oxidation hotspots are present in duplicate. Relative values from the theoretical simulation are compared with experimentally derived values. Clearance for the 3 Met252 oxidation variants is compared with mAb1 control.<sup>1</sup> Relative peak areas in mAb1\_Ox FcRn chromatogram (Fig. 6).<sup>2</sup> According to peptide map and plasmin digest/ESI-MS analysis (Table 1, Figure 6).<sup>3</sup> Simulation for 41% oxMet252 (acc. to Ionescu et al.<sup>23</sup>); reaction rates  $k_{\text{oxMet252}} = 0.19 \text{ h}^{-1}$  and  $k_{\text{oxMet428}} = 0.09 \text{ h}^{-1}$  (acc. to Pan et al.<sup>9</sup>).<sup>4</sup> Assuming binomial distribution of oxMet428 vs Met428 within the 3 isolated peaks, the variant distribution in mAb1\_Ox can be calculated from the total oxMet428 content (peptide map) and the rel. peak areas (Table 1 and Figure 6). For example, for variant mAb1\_Ox\_main peak\_oxMet428/Met428 (in bold): 2 (HC isomers, one oxMet428 on left or on right HC)  $\times$  0.2 (oxMet428 content in mAb1\_Ox\_main peak)  $\times$  0.8 (Met428 content in mAb1\_Ox\_main peak)  $\times$  0.3 (rel. peak area of mAb1\_Ox\_main peak in FcRn chromatogram)  $\times$  100 = ~10%.

these three peaks, the Met428/oxMet428 distribution can be easily calculated from the peptide map data assuming a binomial distribution (Scheme 1). Indeed, when comparing the relative quantities of the 10 oxidation variants of mAb1\_Ox derived from our experimental data set with the simulation performed according to Ionescu et al.,<sup>23</sup> a good agreement of the results is observed. The reaction rates for the oxidation used for this simulation were 0.19 h<sup>-1</sup> and 0.09 h<sup>-1</sup> for Met252 and Met428 oxidation, respectively.<sup>9</sup> Notable discrepancies between the experimental and simulated values were observed mainly for the three highly oxidized species containing three or four oxidized methionines. Discrepancies may be due to the negligence of structural changes induced by oxidation at one position that lead to altered reaction rates for the remaining three methionines in the simulation model.

It is noteworthy that only the clearance of the oxMet252/oxMet252 antibody variants (equivalent to mAb1\_Ox\_prepeak II) was significantly faster with a factor of ~2 compared with untreated mAb1 in this study. The half-lives of the other variants that contain no or only one oxMet252 per IgG were not significantly decreased. This means that the exposure of the oxMet252/oxMet252 species was still ~50% of that obtained for mAb1 control. In comparison, the exposure of the other variants was at least 100% compared with mAb1. According to these observations, it should be sufficient to consider the relative content of the oxMet252/oxMet252 species, determined either by FcRn chromatography or by calculation from peptide map data assuming a binomial distribution of oxMet252 and Met252, in order to estimate the PK properties of an antibody batch, e.g., after extended storage.

In mAb1\_Ox, the relative content of the oxMet252/oxMet252 variant was determined to be 20% using FcRn chromatography, whereas 80% of molecules were oxMet252/Met252 and Met252/Met252 variants (both exhibiting 100% exposure). Since the 20% oxMet252/oxMet252 variant still conveyed half of the exposure of unmodified IgG, it is comprehensible why the exposure of mAb1\_Ox was not significantly lower than that of mAb1 in our study despite of the high overall Met252 and Met428 oxidation levels.

Thus, IgG batches with a total oxMet252 level of ~40% (e.g., mAb1\_Ox) contain ~80% molecules that have at least one HC intact and are able to bind to FcRn.

These considerations are in agreement with previous PK studies conducted in huFcRn-transgenic mice, where such oxidized antibody preparations exhibited similar PK properties as the unmodified control sample.<sup>8</sup> A markedly deteriorated PK profile was only observed after the oxMet252 content was increased to 80% by extended incubation with hydrogen peroxide.<sup>8</sup>

Considering that the levels of Fc methionine oxidation after hydrogen peroxide treatment as applied in our study and in the literature (e.g., Wang et al.<sup>8</sup>) are far higher than those typically observed during normal refrigerated shelf-life, it appears unlikely that overall PK properties of therapeutic antibody preparations will be negatively affected by oxidation events.

## Conclusion

Three main antibody oxidation variants were isolated from a hydrogen peroxide-treated IgG batch based on their different FcRn binding properties utilizing the novel pH gradient FcRn affinity chromatography as a preparative tool. By this approach we were able to isolate and characterize antibody oxidation variants differing in the content of oxMet252 and, to a lesser extent, oxMet428 for the first time. FcRn/IgG interaction characteristics in the FcRn chromatography were confirmed by SPR analysis and have been shown to be predictive of FcRn-mediated PK properties *in vivo*. Met252 oxidation was the dominant contributor to PK impairment observed in mice transgenic for the human FcRn receptor. Importantly, increased plasma clearance was only observed if both IgG HCs were oxidized at Met252. The effect of Met428 oxidation on FcRn binding is most probably subordinate to the dominant chemical/structural changes due to Met252 oxidation, but may amplify this negative effect if co-localized.

Overall, the results presented here suggest that the relevance of methionine oxidation for the FcRn-dependent PK properties of therapeutic antibodies may have been overestimated, and that a very high oxidation threshold has to be exceeded (~>50% oxMet252) before markedly faster plasma clearance is observed *in vivo*.

## Materials and Methods

### Sample preparation

Approximately 200 mg of a representative humanized monoclonal IgG1 (G1m1,17 allotype) from the Roche development portfolio were treated with 0.01% (v/v) hydrogen peroxide for 18 h according to published protocols to induce methionine oxidation in the Fc.<sup>7</sup> The oxidation reaction was quenched by addition of 50 mM L-methionine solution. The original untreated antibody batch was termed mAb1, whereas the H<sub>2</sub>O<sub>2</sub>-treated portion of the batch was named mAb1\_Ox.

The FcRn affinity chromatography method was described previously.<sup>27</sup> For preparative purposes, 60 mg FcRn/ $\beta$ 2-microglobulin were expressed, purified and biotinylated as described. For coupling, 10 g streptavidin sepharose (GE Healthcare) were added to the prepared receptor and incubated for two hours at room temperature under mild shaking. The resulting FcRn-sepharose matrix was filled in a XK 16 column housing (W 1.6 cm  $\times$  L 6 cm, GE Healthcare) and incorporated in an ÄKTA Avant chromatography system (GE Healthcare). The column was equilibrated with 20 mM 2-(N-morpholine)-ethanesulfonic acid (MES) buffer containing 150 mM NaCl, pH 5.5 (eluent A) at a flow rate of 2 ml/min.

The oxidized antibody sample mAb1\_Ox containing ~20 mg of IgG was adjusted to pH 5.5 by dilution with eluent A and applied to the FcRn column at room temperature. The column was washed with 5 column volumes of eluent A followed by elution of the bound antibody in a linear gradient from 0–100% 20 mM Tris/HCl, 150 mM NaCl, pH 8.5 (eluent B) in 40 column volumes. The elution profile was obtained by continuous

measurement of the absorbance at 280 nm. The eluate was collected in 4 ml fractions that were pooled as depicted in Figure 3C, resulting in three samples: mAb1\_Ox\_prepeak II, mAb1\_Ox\_prepeak I and mAb1\_Ox\_main peak (in sequence of elution). In order to obtain sufficient quantities of all three separated antibody oxidation variants for the intended characterization, fractions of eight separation runs were collected, pooled and concentrated to ~1 mg/ml using 15 ml Amicon Ultra centrifugal filters (10 kD, Millipore). All five resulting samples (mAb1, mAb1\_Ox, mAb1\_Ox\_main peak, mAb1\_Ox\_prepeak I and mAb1\_Ox\_prepeak II) were subsequently dialyzed against the formulation buffer for mAb1: 20 mM sodium citrate, 190 mM sucrose, 20 mM L-arginine, 0.02% polysorbate 20, pH 5.5, supplemented with 5 mM L-methionine. Protein concentration was adjusted to 1 mg/ml in all samples and aliquots were stored at -70 °C until use.

#### Analytical FcRn chromatography

Separation and sample homogeneity after the preparative FcRn chromatography runs were confirmed for all five samples by analytical scale FcRn affinity chromatography. For this, FcRn-sepharose matrix was filled in a MonoQ column housing (inner diameter 5 mm × length 50 mm, GE Healthcare) and incorporated in a HPLC system with UV detector. The column was equilibrated with 20 mM 2-(N-morpholine)-ethanesulfonic acid (MES) buffer containing 150 mM NaCl, pH 5.5 (eluent A) at 0.3 ml/min. Thirty µg of each sample were diluted at a volume ratio of 1:1 with eluent A and applied to the FcRn column at room temperature. The column was washed with 5 column volumes of eluent A followed by elution in a linear gradient from 0–100% 20 mM Tris/HCl, 150 mM NaCl, pH 8.5 (eluent B) in 36 column volumes. The elution profile was obtained by continuous measurement of the absorbance at 280 nm.

The five samples (mAb1, mAb1\_Ox, mAb1\_Ox\_main peak, mAb1\_Ox\_prepeak I and mAb1\_Ox\_prepeak II) intended for PK evaluation were subjected to a full physico-chemical and functional characterization *in vitro*.

#### Physico-chemical and functional characterization

For determination of protein concentration, dilutions of the generated samples were performed with placebo buffer on an analytical balance at room temperature. Weights of used sample aliquots and diluted samples were recorded with four decimal places. For each sample, three independent dilutions were performed and analyzed in a qualified UV spectrophotometer at 280 nm and 320 nm. After subtracting the absorbance of 320 nm, from the 280 nm absorbance, the protein concentration was calculated according to Lambert-Beer law using the dilution factors and averaging the concentrations obtained from the three independent dilutions per sample. Concentrations were reported with two decimals. Furthermore, the following analytical methods were applied: Size-exclusion chromatography, non-gel sieving denaturing capillary electrophoresis (CE-SDS; non-reduced and reduced), capillary isoelectric focusing (CE-IEF), reverse-phase UPLC of released and labeled oligosaccharides, mAb1-specific SPR target binding assay and mAb1-specific qualified

cell-based functional assay (the latter two assays were developed in-house).<sup>38–44</sup> The five samples were comparable with regard to quality and physico-chemical properties by using the above mentioned analytical methods, e.g., very low aggregate content, unaltered charge distribution, identical oligosaccharide profiles, *in vitro* target binding and functionality (data not shown).

#### Tryptic peptide mapping by RP-HPLC-MS/MS

An aliquot of 190 µL 8M guanidine hydrochloride/0.4 M tris (hydroxymethyl)aminomethane hydrochloride (TRIS-HCl), pH 8.0 was added to 50 µg protein in 50 µL formulation buffer and incubated for 1 h at 37 °C with 20 µL 0.24 M dithiothreitol (DTT). Subsequently the mixture was incubated with 20 µL 0.6 M iodoacetic acid for 0.25 h at room temperature in the dark. Reaction was quenched by addition of 30 µL 0.24 M DTT. The sample was transferred into 482 µL 50 mM TRIS-HCl by buffer exchange on a Sephadex G25 column. For tryptic digests, 13.4 µL trypsin (Promega, sequencing grade) (0.25 mg/mL trypsin in 50 mM TRIS-HCl) were added. The addition of trypsin was repeated after 2.5 h, the total incubation time was 5 h at 37 °C and the final mAb1/trypsin ratio ~36:1 (w/w). For quenching, 20 µL 10% formic acid were added. The sample was centrifuged at 9,000 g for 5 min. An ACQUITY nanoUPLC (Waters) running in „high flow mode” followed by a Triversa Nanomate nanoESI-source (Advion) and coupled with a LTQ-Orbitrap (Thermo) was used for sample analysis. Four µl of sample were loaded onto a ACQUITY UPLC column (BEH300 C18, 1.0 × 150 mm, 1.7 µm) using a flow rate of 60 µl/min, a column temperature of 50 °C and a gradient of 1 to 40% eluent B (0.1% formic acid/acetoneitrile) in 130 min (eluent A: 0.1% formic acid). Data analysis was performed using the XCalibur software (Thermo). The extent of oxidation of a peptide was estimated in a relative manner to the unmodified peptide using this software.

#### Electrospray ionization mass spectrometry (ESI-MS) after plasmin digest

For mass spectrometry analysis of the Fc, a plasmin digest was performed. For the digest, 100 µg of all five samples were dialyzed using slide-a-lyzers into 50 mM Tris(hydroxymethyl)aminomethane, pH 8.0, at 4 °C overnight. Subsequently, 0.1 units plasmin (1.05 U plasmin/mg Protein, Roche Diagnostics) were added to each sample and incubated at 25 °C for 72 h. After the digest, plasmin-treated samples (50 µg) were deglycosylated by adding 0.5 µL N-glycanase plus (Roche Diagnostics) and sodium phosphate buffer (0.1 M, pH 7.1) to obtain a final sample volume of 115 µL. The mixture was incubated at 37 °C for 18 h. For denaturing, 100 µL of 6 M Gua-HCl (Pierce) were added. The mixture was incubated at 37 °C for 30 min. Samples were desalted by SEC (Sephacrose G-25, isocratic, 40% acetoneitrile with 2% formic acid). ESI mass spectra (+ve) were recorded on a Q-TOF instrument (maXis, Bruker) equipped with a nano ESI source (TriVersa NanoMate, Advion). MS parameter settings were as follows: Transfer: Funnel RF, 400 Vpp; ISCID Energy, 0 eV; Multipole RF, 400 Vpp; Quadrupole: Ion Energy, 4.0 eV; Low Mass, 600 m/z; Source: Dry Gas, 8 L/min; Dry Gas Temperature, 160 °C; Collision Cell: Collision Energy,

10 eV; Collision RF: 2000 Vpp; Ion Cooler: Ion Cooler RF, 300 Vpp; Transfer Time: 120  $\mu$ s; Pre Puls Storage, 10  $\mu$ s; scan range m/z 600 to 2000. Software (MassAnalyzer) developed in-house was used for data evaluation.

### Surface plasmon resonance analysis – FcRn binding

The FcRn binding properties of mAb1 starting material were compared with that of the other four samples by SPR technology using a BiaCore T100 instrument (BiaCore AB). FcRn receptor was immobilized on a Biacore CM5-biosensor chip (GE Healthcare Bioscience) via amine coupling to a level of 400 response units (RU). The assay was performed at room temperature with PBS, 0.05% polysorbate 20, pH 6.0 (GE Healthcare Bioscience) as running and dilution buffer. A total of 200 nM of each antibody sample were injected at a flow rate of 50  $\mu$ L/min at room temperature. Association time was 180 s, dissociation phase was 360 s. Regeneration of the chip surface was accomplished by a short injection of HBS-P, pH 8.0. Evaluation of SPR-data was performed by comparing the response signal height at 180 s after injection and the dissociation behavior by overlay. The corresponding parameters are the RU max level (180 s after injection) and a sensorgram alignment. The RU max values were calculated in relative difference values to the reference mAb1 material.

### Pharmacokinetic study in human FcRn-transgenic mice

Female C57BL/6J mice deficient in mouse FcRn  $\alpha$  chain gene, but hemizygous transgenic for a human FcRn  $\alpha$ -chain gene (mFcRn $-/-$  huFcRn tg +/-, line 276; Jackson Laboratories, Bar Harbor, USA) were used throughout the PK studies.<sup>45,46</sup> Procedures were performed in accordance with the guidelines of the Association for Assessment and Accreditation of Laboratory Animal Care (<http://www.aaalac.org>). All studies were authorized by the Regional Council of Oberbayern, Germany.

The five antibody samples were given as a single intravenous bolus injection via the tail vein. Due to limited blood volume of mice, three groups of six animals each were required to cover nine sampling time points, i.e., three sampling time points per animal. Blood samples were taken in group 1 at 5 min, 24 and 336 h, in group 2 at 2, 168 and 504 h, and in group 3 at 8, 48, and 672 h after administration. Blood samples of about 100  $\mu$ L were obtained by retrobulbar puncture and stored at room temperature for 60 min to allow clotting. Serum samples of at least 40  $\mu$ L were obtained by centrifugation at 9300 x g at 4 °C for 3 min and immediately frozen and stored at -20 °C until analyzed.

### References

1. Buss NA, Henderson SJ, McFarlane M, Shenton JM, de Haan L. Monoclonal antibody therapeutics: history and future. *Curr Opin Pharmacol* 2012; 12:615-22; PMID:22920732; <http://dx.doi.org/10.1016/j.coph.2012.08.001>
2. Reichert JM. Antibodies to watch in 2013: Mid-year update. *MAbs* 2013; 5:513-7; PMID:23727858; <http://dx.doi.org/10.4161/mabs.24990>
3. Chan AC, Carter PJ. Therapeutic antibodies for autoimmunity and inflammation. *Nat Rev Immunol* 2010;

- 10:301-16; PMID:20414204; <http://dx.doi.org/10.1038/nri2761>
4. Nimmerjahn F, Ravetch JV. Fc $\gamma$  receptors as regulators of immune responses. *Nat Rev Immunol* 2008; 8:34-47; PMID:18064051; <http://dx.doi.org/10.1038/nri2206>
5. Roopenian DC, Akilish S. FcRn: the neonatal Fc receptor comes of age. *Nat Rev Immunol* 2007; 7:715-25; PMID:17703228; <http://dx.doi.org/10.1038/nri2155>
6. Nelson AL, Dhimolea E, Reichert JM. Development trends for human monoclonal antibody therapeutics.

Serum levels of the five antibody samples were determined by a mAb1-antigen-captured electrochemiluminescence immunoassay using the ELECSYS e411 immunoanalyzer (Roche Diagnostics). Briefly, serum samples, undiluted or pre-diluted with assay buffer, were incubated with capture and detection molecules for 9 min at 37 °C. Biotinylated recombinant mAb1 antigen was used as capture molecule and a ruthenium(II) tris (bipyridyl)<sub>3</sub><sup>2+</sup> (Ru[bpy]<sub>3</sub><sup>2+</sup>) labeled anti-Ab1-idiotype mouse monoclonal antibody was used for detection. Streptavidin-coated magnetic microparticles were added and incubated for additional 9 min at 37 °C to allow complex formation due to biotin-streptavidin interactions. Complexes are magnetically captured on an electrode and a chemiluminescent signal generated using the co-reactant tripropylamine (TPA) was measured by a photomultiplier detector. All serum samples and positive or negative control samples were analyzed in replicates and calibrated against reference standard.

PK parameters were calculated by non-compartmental analysis, using the PK evaluation program WinNonlin<sup>TM</sup> (Pharsight), version 5.2.1. Briefly, the area under the concentration/time curve AUC (0–672 h) was calculated by linear trapezoidal rule (with linear interpolation) from time 0 to infinity. The apparent terminal half-life ( $t_{1/2}$ ) was derived from the equation:  $t_{1/2} = \ln 2 / \lambda_z$ . Total body clearance (CL) was calculated as Dose/AUC. Statistically significant differences in the PK parameters between different mAb1 preparations were determined by ANOVA analysis.

### Disclosure of Potential Conflicts of Interest

All authors are current or former employees of Roche Diagnostics GmbH.

### Acknowledgments

We thank Isabel Hermann, Andreas Petzold, Adrian Zwick and Simone Lutz for contributing to the sample characterization. Hans Auer and Stefan Seeber have kindly provided the FcRn. All above colleagues are or were part of Roche Research and Early Development (pRED), Roche Innovation Center Penzberg, Germany. Ulla Grauschopf (Pharmaceutical Development and Supplies, Roche, Basel, Switzerland) kindly supported the study with thermal stability data of an oxidized full-length antibody.

### Supplemental Material

Supplemental data for this article can be accessed on the publisher's website.

- Nat Rev Drug Discov 2010; 9:767-74; PMID:20811384; <http://dx.doi.org/10.1038/nrd3229>
7. Bertolotti-Ciarlet A, Wang W, Lownes R, Pristatsky P, Fang Y, McKelvey T, Li Y, Li Y, Drummond J, Prueksaritanont T, et al. Impact of methionine oxidation on the binding of human IgG1 to Fc Rn and Fc gamma receptors. *Mol Immunol* 2009; 46:1878-82; PMID:19269032; <http://dx.doi.org/10.1016/j.molimm.2009.02.002>
8. Wang W, Vlasak J, Li Y, Pristatsky P, Fang Y, Pittman T, Roman J, Wang Y, Prueksaritanont T, Ionescu R.

- Impact of methionine oxidation in human IgG1 Fc on serum half-life of monoclonal antibodies. *Mol Immunol* 2011; 48:860-6; PMID:21256596; <http://dx.doi.org/10.1016/j.molimm.2010.12.009>
9. Pan H, Chen K, Chu L, Kinderman F, Apostol I, Huang G. Methionine oxidation in human IgG2 Fc decreases binding affinities to protein A and FcRn. *Protein Sci* 2009; 18:424-33; PMID:19165723; <http://dx.doi.org/10.1002/pro.45>
  10. Thirumangalathu R, Krishnan S, Bondarenko P, Speed-Ricci M, Randolph TW, Carpenter JF, Brems DN. Oxidation of methionine residues in recombinant human interleukin-1 receptor antagonist: implications of conformational stability on protein oxidation kinetics. *Biochemistry* 2007; 46:6213-24; PMID:17480058; <http://dx.doi.org/10.1021/bi700321g>
  11. Rao PE, Kroon DJ. Orthoclone OKT3. Chemical mechanisms and functional effects of degradation of a therapeutic monoclonal antibody. *Pharm Biotechnol* 1993; 5:135-58; PMID:8019692; [http://dx.doi.org/10.1007/978-1-4899-1236-7\\_4](http://dx.doi.org/10.1007/978-1-4899-1236-7_4)
  12. Martin WL, West AP Jr., Gan L, Bjorkman PJ. Crystal structure at 2.8 Å of an FcRn/heterodimeric Fc complex: mechanism of pH-dependent binding. *Mol Cell* 2001; 7:867-77; PMID:11336709; [http://dx.doi.org/10.1016/S1097-2765\(01\)00230-1](http://dx.doi.org/10.1016/S1097-2765(01)00230-1)
  13. Goebel NA, Babbey CM, Datta-Mannan A, Witcher DR, Wroblewski VJ, Dunn KW. Neonatal Fc receptor mediates internalization of Fc in transfected human endothelial cells. *Mol Biol Cell* 2008; 19:5490-505; PMID:18843053; <http://dx.doi.org/10.1091/mbc.E07-02-0101>
  14. Ward ES, Martinez C, Vaccaro C, Zhou J, Tang Q, Ober RJ. From sorting endosomes to exocytosis: association of Rab4 and Rab11 GTPases with the Fc receptor, FcRn, during recycling. *Mol Biol Cell* 2005; 16:2028-38; PMID:15689494; <http://dx.doi.org/10.1091/mbc.E04-08-0735>
  15. Sánchez LM, Penny DM, Bjorkman PJ. Stoichiometry of the interaction between the major histocompatibility complex-related Fc receptor and its Fc ligand. *Biochemistry* 1999; 38:9471-6; PMID:10413524; <http://dx.doi.org/10.1021/bi9907330>
  16. Edelman GM, Cunningham BA, Gall WE, Gottlieb PD, Rutishauser U, Waxdal MJ. The covalent structure of an entire gammaG immunoglobulin molecule. *Proc Natl Acad Sci U S A* 1969; 63:78-85; PMID:5257969; <http://dx.doi.org/10.1073/pnas.63.1.78>
  17. Jefferis R, Lefranc MP. Human immunoglobulin allotypes: possible implications for immunogenicity. *MAbs* 2009; 1:332-8; PMID:20073133; <http://dx.doi.org/10.4161/mabs.1.4.9122>
  18. Shen FJ, Kwong MY, Keck RG, Harris RJ. The application of tert-butylhydroperoxide oxidation to study sites of potential methionine oxidation in a recombinant antibody. *Tech Protein Chem* 1996; 7:275-84; [http://dx.doi.org/10.1016/S1080-8914\(96\)80031-7](http://dx.doi.org/10.1016/S1080-8914(96)80031-7)
  19. Burkitt W, Domann P, O'Connor G. Conformational changes in oxidatively stressed monoclonal antibodies studied by hydrogen exchange mass spectrometry. *Protein Sci* 2010; 19:826-35; PMID:20162626; <http://dx.doi.org/10.1002/pro.362>
  20. Houde D, Peng Y, Berkowitz SA, Engen JR. Post-translational modifications differentially affect IgG1 conformation and receptor binding. *Mol Cell Proteomics* 2010; 9:1716-28; PMID:20103567; <http://dx.doi.org/10.1074/mcp.M900540-MCP200>
  21. Wang S, Ionescu R, Peekhaus N, Leung JY, Ha S, Vlasak J. Separation of post-translational modifications in monoclonal antibodies by exploiting subtle conformational changes under mildly acidic conditions. *J Chromatogr A* 2010; 1217:6496-502; PMID:20828701; <http://dx.doi.org/10.1016/j.chroma.2010.08.044>
  22. Liu D, Ren D, Huang H, Dankberg J, Rosenfeld R, Cocco MJ, Li L, Brems DN, Remmele RL Jr. Structure and stability changes of human IgG1 Fc as a consequence of methionine oxidation. *Biochemistry* 2008; 47:5088-100; PMID:18407665; <http://dx.doi.org/10.1021/bi702238b>
  23. Ionescu R, Vlasak J. Kinetics of chemical degradation in monoclonal antibodies: relationship between rates at the molecular and peptide levels. *Anal Chem* 2010; 82:3198-206; PMID:20302349; <http://dx.doi.org/10.1021/ac902752e>
  24. Lam XM, Yang JY, Cleland JL. Antioxidants for prevention of methionine oxidation in recombinant monoclonal antibody HER2. *J Pharm Sci* 1997; 86:1250-5; PMID:9383735; <http://dx.doi.org/10.1021/js970143s>
  25. Gaza-Bulsecu G, Faldu S, Hurkmans K, Chumsae C, Liu H. Effect of methionine oxidation of a recombinant monoclonal antibody on the binding affinity to protein A and protein G. *J Chromatogr B Analyt Technol Biomed Life Sci* 2008; 870:55-62; PMID:18567545; <http://dx.doi.org/10.1016/j.jchromb.2008.05.045>
  26. Hinton PR, Xiong JM, Johlf MG, Tang MT, Keller S, Tsurushita N. An engineered human IgG1 antibody with longer serum half-life. *J Immunol* 2006; 176:346-56; PMID:16365427; <http://dx.doi.org/10.4049/jimmunol.176.1.346>
  27. Schlothauer T, Rueger P, Stracke JO, Hertenberger H, Fingas F, Kling L, Emrich T, Drabner G, Seeber S, Auer J, et al. Analytical FcRn affinity chromatography for functional characterization of monoclonal antibodies. *MAbs* 2013; 5:576-86; PMID:23765230; <http://dx.doi.org/10.4161/mabs.24981>
  28. Huber AH, Kelley RF, Gastinel LN, Bjorkman PJ. Crystallization and stoichiometry of binding of a complex between a rat intestinal Fc receptor and Fc. *J Mol Biol* 1993; 230:1077-83; PMID:8478919; <http://dx.doi.org/10.1006/jmbi.1993.1220>
  29. Ober RJ, Radu CG, Ghetie V, Ward ES. Differences in promiscuity for antibody-FcRn interactions across species: implications for therapeutic antibodies. *Int Immunol* 2001; 13:1551-9; PMID:11717196; <http://dx.doi.org/10.1093/intimm/13.12.1551>
  30. Harris RJ, Kabakoff B, Macchi FD, Shen FJ, Kwong M, Andya JD, Shire SJ, Bjork N, Totpal K, Chen AB. Identification of multiple sources of charge heterogeneity in a recombinant antibody. *J Chromatogr B Biomed Sci Appl* 2001; 752:233-45; PMID:11270864; [http://dx.doi.org/10.1016/S0378-4347\(00\)00548-X](http://dx.doi.org/10.1016/S0378-4347(00)00548-X)
  31. Khawli LA, Goswami S, Hutchinson R, Kwong ZW, Yang J, Wang X, Yao Z, Sreedhara A, Cano T, Tesar D, et al. Charge variants in IgG1: Isolation, characterization, *in vitro* binding properties and pharmacokinetics in rats. *MAbs* 2010; 2:613-24; PMID:20818176; <http://dx.doi.org/10.4161/mabs.2.6.13333>
  32. Loew C, Knoblich C, Fichtl J, Alt N, Diepold K, Bulau P, Goldbach P, Adler M, Mahler HC, Grauschopf U. Analytical protein A chromatography as a quantitative tool for the screening of methionine oxidation in monoclonal antibodies. *J Pharm Sci* 2012; 101:4248-57; PMID:22899501; <http://dx.doi.org/10.1002/jps.23286>
  33. Kamei DT, Lao BJ, Ricci MS, Deshpande R, Xu H, Tidor B, Lauffenburger DA. Quantitative methods for developing Fc mutants with extended half-lives. *Bio-technol Bioeng* 2005; 92:748-60; PMID:16136591; <http://dx.doi.org/10.1002/bit.20624>
  34. Kuo TT, Aveson VG. Neonatal Fc receptor and IgG-based therapeutics. *MAbs* 2011; 3:422-30; PMID:22048693; <http://dx.doi.org/10.4161/mabs.3.5.16983>
  35. Martin WL, Bjorkman PJ. Characterization of the 2:1 complex between the class I MHC-related Fc receptor and its Fc ligand in solution. *Biochemistry* 1999; 38:12639-47; PMID:10504233; <http://dx.doi.org/10.1021/bi9913505>
  36. Petkova SB, Akilesh S, Sproule TJ, Christianson GJ, Al Khabbaz H, Brown AC, Presta LG, Meng YG, Roopenian DC. Enhanced half-life of genetically engineered human IgG1 antibodies in a humanized FcRn mouse model: potential application in humorally mediated autoimmune disease. *Int Immunol* 2006; 18:1759-69; PMID:17077181; <http://dx.doi.org/10.1093/intimm/dxl110>
  37. Zalevsky J, Chamberlain AK, Horton HM, Karki S, Leung IW, Sproule TJ, Lazar GA, Roopenian DC, Desjarlais JR. Enhanced antibody half-life improves *in vivo* activity. *Nat Biotechnol* 2010; 28:157-9; PMID:20081867; <http://dx.doi.org/10.1038/nbt.1601>
  38. Lu C, Liu D, Liu H, Motchnik P. Characterization of monoclonal antibody size variants containing extra light chains. *MAbs* 2013; 5:102-13; PMID:23255003; <http://dx.doi.org/10.4161/mabs.22965>
  39. Michels DA, Brady LJ, Guo A, Balland A. Fluorescent derivatization method of proteins for characterization by capillary electrophoresis-sodium dodecyl sulfate with laser-induced fluorescence detection. *Anal Chem* 2007; 79:5963-71; PMID:17591753; <http://dx.doi.org/10.1021/ac070552i>
  40. Michels DA, Tu AW, McElroy W, Voehringer D, Salas-Solano O. Charge heterogeneity of monoclonal antibodies by multiplexed imaged capillary isoelectric focusing immunoassay with chemiluminescence detection. *Anal Chem* 2012; 84:5380-6; PMID:22663182; <http://dx.doi.org/10.1021/ac3008847>
  41. Wu XZ, Pawliszyn J. Whole-column imaging capillary electrophoresis of proteins with a short capillary. *Electrophoresis* 2002; 23:542-9; PMID:11870762; [http://dx.doi.org/10.1002/1522-2683\(200202\)23:4<542::AID-ELPS542>3.0.CO;2-B](http://dx.doi.org/10.1002/1522-2683(200202)23:4<542::AID-ELPS542>3.0.CO;2-B)
  42. Wu J, Li SC, Watson A. Optimizing separation conditions for proteins and peptides using imaged capillary isoelectric focusing. *J Chromatogr A* 1998; 817:163-71; PMID:9764490; [http://dx.doi.org/10.1016/S0021-9673\(98\)00326-4](http://dx.doi.org/10.1016/S0021-9673(98)00326-4)
  43. Prater BD, Connelly HM, Qin Q, Cockrill SL. High-throughput immunoglobulin G N-glycan characterization using rapid resolution reverse-phase chromatography tandem mass spectrometry. *Anal Biochem* 2009; 385:69-79; PMID:19000897; <http://dx.doi.org/10.1016/j.ab.2008.10.023>
  44. Wuhler M, Koeleman CA, Deelder AM. Two-dimensional HPLC separation with reverse-phase-nano-LC-MS/MS for the characterization of glycan pools after labeling with 2-aminobenzamide. *Methods Mol Biol* 2009; 534:79-91; PMID:19277534
  45. Roopenian DC, Christianson GJ, Sproule TJ, Brown AC, Akilesh S, Jung N, Petkova S, Avanesian L, Choi EY, Shaffer DJ, et al. The MHC class I-like IgG receptor controls perinatal IgG transport, IgG homeostasis, and fate of IgG-Fc-coupled drugs. *J Immunol* 2003; 170:3528-33; PMID:12646614; <http://dx.doi.org/10.4049/jimmunol.170.7.3528>
  46. Roopenian DC, Christianson GJ, Sproule TJ. Human FcRn transgenic mice for pharmacokinetic evaluation of therapeutic antibodies. *Methods Mol Biol* 2010; 602:93-104; PMID:20012394; [http://dx.doi.org/10.1007/978-1-60761-058-8\\_6](http://dx.doi.org/10.1007/978-1-60761-058-8_6)